

This Research Contribution is in Commemoration of the Life and Science of I. M. Kolthoff (1894–1993).

Disproportionation During Electrooxidation of Catecholamines at Carbon-Fiber Microelectrodes

Edward L. Clolkowski, Karolyn M. Maness, Paula S. Cahill, and R. Mark Wightman*

Department of Chemistry, University of North Carolina at Chapel Hill, Chapel Hill, North Carolina 27599-3290

Dennis H. Evans

Department of Chemistry and Biochemistry, University of Delaware, Newark, Delaware 19716

Bruno Fosset and Christian Amatore

Departement de Chimie URA CNRS 1679, Ecole Normale Supérieure, 24 Rue Lhomond, 75231 Paris, France

The effect of following chemical reactions during chronoamperometry and cyclic voltammetry at microelectrodes has been evaluated by digital simulation and the results have been compared to experiments. This study was motivated by the demonstrated utility of microelectrodes to monitor catecholamine secretion from individual biological cells. Since following chemical reactions can increase the total number of coulombs passed, such an occurrence can affect the calibration of the measured response. However, at microelectrodes, products formed by chemical reactions after electron transfer are less likely to return to the electrode because of the divergent diffusion field that can exist at electrodes of small dimensions. The degree to which these effects are apparent has been evaluated quantitatively by digital simulation of the DISP1 scheme for a disk-shaped electrode. The predictions of the simulation are verified in an experimental study of the anodic oxidation of diphenylanthracene in acetonitrile containing pyridine. In contrast, the DISP1 reaction of catecholamines at carbon-fiber microelectrodes exhibits much less enhanced current than predicted by theory. The experimental data suggest this is due to the heterogeneous nature of the carbon surface with respect to electron transfer. Thus, for most applications of carbon-fiber microelectrodes as sensors of catecholamine secretion from cells, the effect of the DISP1 reaction can be ignored.

The catecholamines, dopamine, epinephrine, and norepinephrine, play an important physiological role as extracellular chemical messengers. Because these compounds are easily oxidized, electrochemical techniques have been used to monitor their concentration in the intact brain^{1,2} and at isolated adrenal medullary cells.^{3,4} At the single-cell level, secretion can be resolved at the level of individual vesicular events resulting from exocytotic fusion of the vesicles with the plasma membrane. Thus, for the first time the so-called "quantal"

unit of biological communication can be chemically monitored. However, to relate the measured electrochemical currents to the quantity of material secreted requires that the electrochemical mechanisms of catecholamine oxidation are thoroughly understood.

The electrochemical oxidation of catecholamines in aqueous solution has been characterized at electrodes of conventional size.⁵ The oxidation proceeds as a two-electron process to form catecholamine *o*-quinones (Figure 1). The *o*-quinone of each precursor contains both an electron-deficient ring and an electron-donating amine. When the amine is deprotonated (pK_a 's of 10.63, 9.78, and 9.90 for dopamine, norepinephrine, and epinephrine, respectively⁶) the molecule can undergo a 1,4 (Michael) addition which results in a cyclization reaction. The resulting product, the leucoaminochrome, is more easily oxidized than the parent catecholamine and can undergo further two-electron oxidation to form the aminochrome. This electrochemical–chemical–electrochemical (ECE) reaction sequence causes the apparent number of electrons consumed during the oxidation of the catecholamines to vary from two to four electrons, depending on the time scale of the observation. In accord with other electrochemical mechanisms of this type,^{7,8} the second oxidation occurs as a homogeneous electron transfer with *o*-quinone in solution, regenerating the catecholamine (a DISP1 reaction).

Each of the aforementioned catecholamines has a different rate for the cyclization reaction. However, these differences in rate cannot be observed through electrochemical measurements of catecholamines at short time scales because the kinetics of the chemical reactions are outrun. Thus, with cyclic voltammetry at a scan rate of 300 V/s the catecholamines appear identical.⁹ However, measurements at slower scan rates at physiological pH⁵ show that the rates of cyclization follow the order dopamine < norepinephrine <

(1) Wightman, R. M.; May, L. J.; Michael, A. C. *Anal. Chem.* **1988**, *60*, 769A–779A.

(2) Adams, R. N. *Prog. Neurobiol.* **1990**, *35*, 297–311.

(3) Leszczyszyn, D. J.; Jankowski, J. A.; Viveros, O. H.; Diliberto, E. J., Jr.; Near, J. A.; Wightman, R. M. *J. Biol. Chem.* **1990**, *265*, 14736–14737.

(4) Wightman, R. M.; Jankowski, J. A.; Kennedy, R. T.; Kawagoe, K. T.; Schroeder, T. J.; Leszczyszyn, D. J.; Near, J. A.; Diliberto, E. J., Jr.; Viveros, O. H. *Proc. Natl. Acad. Sci. U.S.A.* **1991**, *88*, 10754–10758.

(5) Hawley, M. D.; Tatawawadi, S. V.; Piekarski, S.; Adams, R. N. *J. Am. Chem. Soc.* **1967**, *89*, 447–450.

(6) Lewis, G. P. *Br. J. Pharmacol.* **1954**, *9*, 488–493.

(7) Hawley, M. D.; Feldberg, S. W. *J. Phys. Chem.* **1966**, *70*, 3459–3464.

(8) Amatore, C.; Saveant, J.-M. *J. Electroanal. Chem.* **1978**, *86*, 227–232. Amatore, C.; Gareil, M.; Saveant, J.-M. *J. Electroanal. Chem.* **1978**, *147*, 1–38.

(9) Baur, J. E.; Kristensen, E. W.; May, L. J.; Wiedemann, D. J.; Wightman, R. M. *Anal. Chem.* **1988**, *60*, 1268–1272.

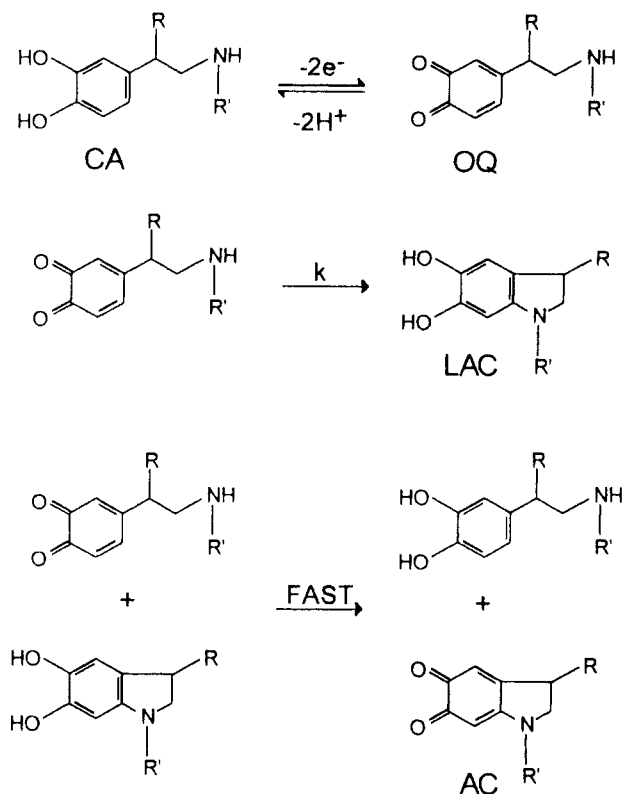


Figure 1. Mechanism of catecholamine disproportionation. For each of the catecholamines, R and R' are, respectively, as follows: dopamine, H, H; norepinephrine, OH, H; epinephrine, OH, CH₃ CA, catecholamine; OQ, o-quinone; LAC, leucoaminochrome; AC, aminochrome.

epinephrine. Prior work has exploited these differences to distinguish between norepinephrine and epinephrine secreted from individual biological cells with carbon-fiber microelectrodes.¹⁰ These studies were complicated by the fact that, at slow time scales, divergent diffusion at microelectrodes removes electrochemically generated products from the vicinity of the electrode, making following chemical reactions more difficult to observe.¹¹ In this respect, microelectrodes are analogous to the rotated disk electrode.^{12,13} However, resolution of the two catecholamines was accomplished by impeding diffusion by the use of a perfluorinated ion exchange membrane on the electrode surface.

In this work we examine the effect of chemical reactions following the initial electron transfer at microelectrodes. This work is motivated by measurements in which carbon-fiber electrodes have been used for amperometric detection of catecholamine secretion from individual adrenal cells. In these experiments, released catecholamines are oxidized following diffusional transport from the cell to the electrode surface. When the collection efficiency has been accounted for,¹⁴ the amount of catecholamine released can be determined by the use of Faraday's law. However, the occurrence of these following chemical reactions, and the uncertainty of the

chemical identity of the catecholamine released, make the assignment of the number of electrons equivocal. This problem is particularly egregious when results obtained at different pH values are compared,¹⁵ since the rate of cyclization of the catecholamines is pH dependent.

For these reasons we have investigated whether the DISP1 reaction could affect the time course and amplitude of the measured spikes. Because a model system to mimic the amperometric detection at cells does not exist, we have instead examined the cyclization of catecholamines at microelectrodes with chronoamperometry and cyclic voltammetry. This enables the time scale of the observable effects of the following chemical reactions to be addressed under conditions of divergent diffusion. The results of the DISP1 simulation are compared to experimental data to evaluate the degree to which the currents at carbon-fiber microelectrodes are affected by the catecholamine disproportionation reaction.

EXPERIMENTAL SECTION

Construction of Microelectrodes. Carbon-fiber microdisk electrodes were fabricated as described previously.¹⁶ Single carbon fibers ($r = 16.5 \mu\text{m}$, Textron Specialty Materials, Lowell, MA, or $r = 5 \mu\text{m}$, Thornell P-55, Amoco Corp., Greenville, SC) were inserted into glass capillaries (6020, A-M Systems, Everett, WA) which were pulled with a pipet puller (Model RF-2, Narishige, Tokyo). The tips were sealed with epoxy (Epon Resin 828, Miller-Stephenson Co., Danbury, CT). Electrodes were polished on a micropipet beveller (Model BV-10, Sutter Instruments, Novato, CA) at a 45° angle, resulting in elliptical tips. The electrodes were stored in 2-propanol until use. The 2-propanol enhances sensitivity and reproducibility, presumably by removing any residual solids that may have adhered to the electrode surface during polishing. Electrical contact to the fiber was made by back-filling the capillary with colloidal graphite (Bio-Rad, Cambridge, MA) and a contact wire.

To fabricate smaller electrodes, a 50–200- μm length of 5- μm -radius fiber was left protruding from the end of the pulled capillary. The tips were dipped in epoxy as above to provide a seal between the glass and the carbon, and excess epoxy was removed with hot toluene. After curing, the tip of the protruding fiber was electrochemically etched to a conical shape,¹⁷ and an insulating polymer (poly(phenylene oxide)) was electrodeposited¹⁸ onto its surface. The tip was exposed by lowering it onto the polishing wheel.

Carbon-fiber electrodes that could be fractured to expose a clean surface were fabricated from the 16.5- μm -radius fibers. A 200–500- μm length of fiber was left protruding from the end of the capillary. The tips were dipped in epoxy and then toluene as described above. After curing, a poly(phenylene oxide) coating was applied to insulate the electrode. For each experiment, the electrode was lowered into the analyte solution and a fresh surface was exposed by trimming the tip of the electrode with a small pair of scissors.

(10) Ciolkowski, E. L.; Cooper, B. R.; Jankowski, J. A.; Jorgenson, J. W.; Wightman, R. M. *J. Am. Chem. Soc.* **1992**, *114*, 2815–2821.
 (11) Dayton, M. A.; Brown, J. C.; Stutts, K. J.; Wightman, R. M. *Anal. Chem.* **1980**, *52*, 946–950.
 (12) Fleischmann, M.; Lasserre, F.; Robinson, J.; Swan, D. J. *Electroanal. Chem.* **1984**, *177*, 97–114.
 (13) Qiankun, Z.; Hongyuan, C. *J. Electroanal. Chem.* **1993**, *346*, 471–475.
 (14) Schroeder, T. J.; Jankowski, J. A.; Kawagoe, K. T.; Wightman, R. M.; Lefrou, C.; Amatore, C. *Anal. Chem.* **1992**, *64*, 3077–3083.

(15) Jankowski, J. A.; Schroeder, T. J.; Ciolkowski, E. L.; Wightman, R. M. *J. Biol. Chem.* **1993**, *268*, 14694–14700.
 (16) Wightman, R. M.; Wipf, D. O. In *Electroanalytical Chemistry*; Bard, A. J., Ed.; Marcel Dekker: New York, 1988; Vol. 17, pp 267–353.
 (17) Kawagoe, K. T.; Jankowski, J. A.; Wightman, R. M. *Anal. Chem.* **1991**, *63*, 1589–1594.
 (18) Potje-Kalmoth, K.; Janata, J.; Josowicz, M. *Ber. Bunsenges. Phys. Chem.* **1989**, *93*, 1480–1485.

Platinum microelectrodes were prepared by sealing platinum wire in soft glass as described previously.¹⁶ Electrodes had nominal radii of 5, 12.5, 25, and 50 μm . Large platinum ($r = 0.82$ mm) and glassy carbon ($r = 1.5$ mm) electrodes were from BioAnalytical Systems (West Lafayette, IN). All of these electrodes were polished with 0.1- μm alumina prior to each experiment and sonicated for 5 min in 50:50 methanol-water to remove residual alumina particles.

Instrumentation. For large electrodes, potentials were generated with a PAR 175 Universal Programmer (EG&G Princeton Applied Research, Princeton, NJ) and employed a home-built potentiostat. All other experiments were performed with an EI-400 potentiostat (Ensmann Instrumentation, Bloomington, IN), displayed on a digital oscilloscope (NIC 310, Nicolet Instruments, Madison, WI) and saved on a floppy disk.

Procedures. Experiments with diphenylanthracene (DPA) were performed in a nitrogen-filled glovebox. Voltammograms and chronoamperograms of DPA were collected in solutions of (A) 0.1 M tetrabutylammonium hexafluorophosphate (TBAH), (B) 0.1 M TBAH and 0.5 mM DPA, and (C) 0.1 M TBAH, 0.5 mM DPA, and 5 mM pyridine. Values of n_{app} were obtained by normalizing the responses obtained in solution C to that in solution B. A silver quasi-reference electrode was employed.

DISP1 rate constants for the catecholamines under conditions of planar diffusion were determined in a phosphate buffer that contained 150 mM sodium chloride. The buffer was adjusted to the desired pH (6.5, 7.4, or 8.0) with either phosphoric acid or sodium hydroxide. Solutions typically contained 1 mM catecholamine and were deoxygenated with nitrogen prior to use. Values of n_{app} were obtained by normalizing the observed value of $it^{1/2}$ to the value calculated from the nominal electrode radius, concentration, and diffusion coefficient for the case where no following chemical reactions occur.

Measurements with carbon-fiber microelectrodes were performed on a vibration-isolation table. Values of n_{app} were determined by normalization of the catecholamine response to the response obtained for 3,4-dihydroxybenzylamine, a catecholamine analogue that cannot undergo a following chemical reaction. A sodium-saturated calomel electrode (SSCE) was used for all aqueous experiments.

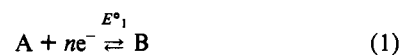
Chemicals. All chemicals were obtained from commercial sources. DPA was recrystallized twice from absolute ethanol. TBAH was dried under vacuum to remove traces of water. Acetonitrile was passed through a column of activated alumina prior to use. Catecholamine stock solutions (10 mM) were prepared in 0.1 N perchloric acid and stored at 4 °C. Phosphate buffer was prepared with doubly distilled water.

Digital Simulation. The chronoamperometric and cyclic voltammetric responses of the DISP1 mechanism at a microdisk were evaluated by digital simulation with the formulation previously described.¹⁹ Simulation of diffusion employed the Hopscotch algorithm²⁰ and was based on a

conformal map²¹ which is suited to the concentration profiles that exist near a microdisk at steady state.

RESULTS AND DISCUSSION

DISP1 Reaction at Microelectrodes. For reactions that involve a chemical reaction and electron transfer following the initial electron transfer, the following general scheme (for a reduction) can be written:⁸



The classical ECE reaction scheme describes the situation where k' is zero. The DISP reactions are operant when reaction 3 does not occur. The DISP1 reaction scheme describes the case where $k_{-1} = 0$, and the forward step in reaction 2 is rate limiting. Alternatively, the DISP2 reaction scheme describes the situation where reaction 4 is rate determining and reaction 2 is in rapid equilibrium. The presence of any of these limiting cases causes an increase in the Faradaic current relative to that found in the absence of a reaction, and this increase is time dependent in the case of chronoamperometry and sweep rate dependent in the case of cyclic voltammetry.^{7,8}

The scheme that best describes the current during the oxidation of catecholamines is the DISP1 reaction scheme. This scheme can be distinguished from the DISP2 scheme since the rate of the latter is dependent on the initial concentration of reactants, a condition not found for these substances (vide infra). In general, the ECE is unlikely during a reduction when $E^{\circ}_2 > E^{\circ}_1$,²² because species C is formed sufficiently far from the electrode that reduction via the exergonic homogeneous electron transfer via reaction 4 is favored.⁸

Under conditions of planar diffusion, the ratio of the current with a DISP1 reaction to that without (n_{app}) during chronoamperometry is given by²³

$$n_{\text{app}} = \frac{\exp(-kt) + 2kt - 1}{kt} \quad (5)$$

However, with a smaller electrode the ratio $(Dt)^{1/2}/r$, where D is the diffusion coefficient and r is the radius of the electrode, increases and conditions of divergent diffusion prevail. Under these conditions, the equivalent time that controls diffusion and chemical reactions is equal to r^2/D . Thus, as r is decreased, the effect of the chemical followup reaction becomes less apparent (Figure 2 shows some examples). This is a consequence of the smaller size of the diffusion layer, which means that there is less time for reactant C to be formed in the vicinity of the electrode. Similar behavior is found for the ECE reaction (see Appendix 1).

(19) Fosset, B.; Amatore, C.; Bartelt, J. E.; Wightman, R. M. *Anal. Chem.* **1991**, *63*, 1403-1408.

(20) Shoup, D.; Szabo, A. *J. Electroanal. Chem.* **1984**, *160*, 1-17.

(21) Amatore, C.; Fosset, B. *J. Electroanal. Chem.* **1992**, *328*, 21-32.

(22) Forno, A. E.; Peover, M. E.; Wilson, R. *Trans. Faraday Soc.* **1970**, *66*, 1322-1333.

(23) Evans, D. H.; Rosanske, T. W.; Jimenez, P. J. *J. Electroanal. Chem.* **1974**, *51*, 449-451.

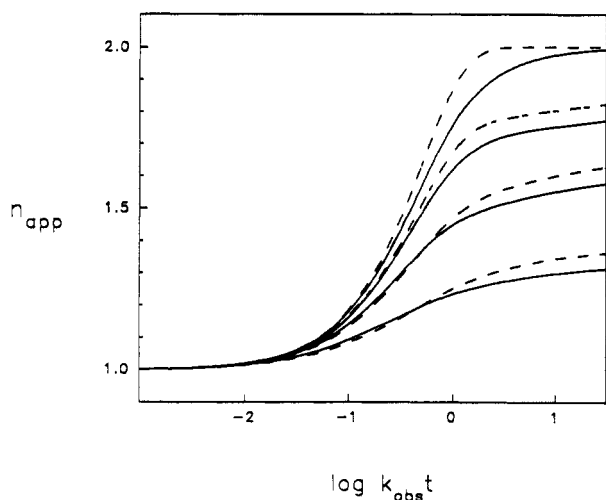


Figure 2. Comparison of DISP1 and ECE chronoamperometric responses at microdisk and hemispherical electrodes. Solid lines correspond to the DISP1 mechanism, dashed lines to the ECE mechanism. The top two traces are for conditions of planar diffusion obtained from eqs 5 and 7. The remaining solid traces were obtained by digital simulation of DISP1 kinetics at a microdisk electrode. Values of kr_0^2/D were 100 (second largest solid trace), 10, and 1 (smallest trace). Dashed lines were obtained by evaluating the analytical solution for ECE kinetics at a hemispherical electrode. For purposes of comparison between the two mechanisms at the two different electrodes, the radii of the disk and hemispherical electrode were made equivalent through the relationship, $r_0 = (2/\pi)r_d$. In addition, the responses of the two mechanisms were overlaid by expressing them as a function of k_{obs} where k_{obs} equals k for the DISP1 reaction mechanism and $1/2k$ for the ECE reaction mechanism, where k is the rate constant for reaction 2.

DISP1 Reaction of Diphenylanthracene Radical Cation with Pyridine. The anodic addition of pyridine to diphenylanthracene follows a DISP1 reaction scheme^{24,25} and was chosen as a model system to compare with the results from the digital simulation of DISP1 kinetics at a microdisk electrode. The pseudo-first-order rate constant for the experimental conditions was first determined by chronoamperometry and cyclic voltammetry with a macroelectrode under conditions of planar diffusion. The chronoamperometric data was fit to eq 5 by nonlinear regression and produced a k value of 26 s^{-1} . The voltammetric data were evaluated with a working curve²⁶ and yielded a value of 20 s^{-1} , in reasonable agreement with the chronoamperometric result.

Cyclic voltammograms were obtained in the same solutions with disk electrodes of smaller dimensions to increase the value of Dt/r^2 . The results are shown in Figure 3 for a scan rate of 100 mV/s . The effects of the chemical followup reaction are apparent with each electrode; however, the increase in current is least apparent with the smallest electrode employed. Overlaid on the data are simulated responses that employed $k = 15 \text{ s}^{-1}$. The reasonable agreement of this value with the values obtained with larger electrodes supports the validity of the simulation.

Disproportionation of Catecholamines at Planar Electrodes. Figure 4A shows a cyclic voltammogram for dopamine obtained at a scan rate of 100 mV/s with a macroelectrode. The initial, positive going scan exhibits a wave for the oxidation

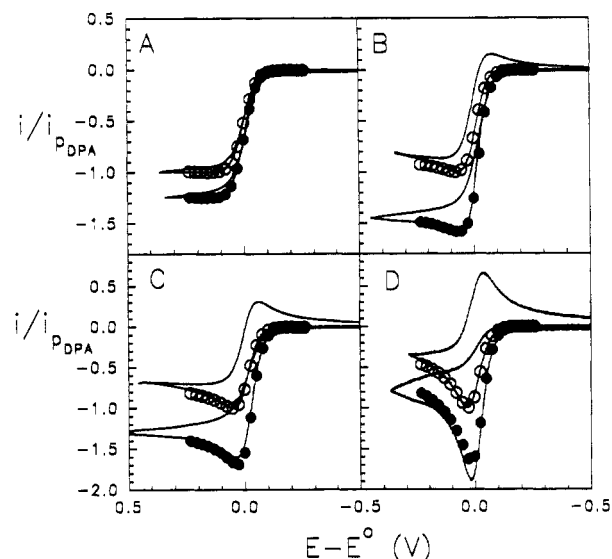


Figure 3. Comparison of data and simulation for the DISP1 reaction of diphenylanthracene (0.5 mM) and pyridine (5 mM) in acetonitrile containing 0.1 M tetrabutylammonium hexafluorophosphate. Scan rate 100 mV/s . Electrode radii were 5 (A), 25 (B), 50 (C), and $820 \mu\text{m}$ (D). Currents have been normalized to the peak oxidative current obtained for diphenylanthracene alone. The simulation employed a DISP1 rate constant of 15 s^{-1} (solid circles). The open circles represent the simulated voltammogram in the absence of following chemical kinetics.

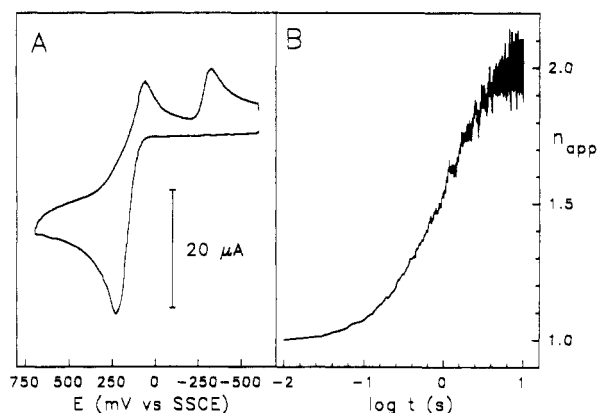


Figure 4. Effects of DISP1 reactions at a glassy carbon electrode under conditions of planar diffusion: (A) cyclic voltammogram of 1 mM dopamine; scan rate 100 mV/s , pH 7.4. Oxidation current is plotted in the downward direction. (B) n_{app} plot for 1 mM norepinephrine, pH 7.4, obtained by chronoamperometry.

of dopamine to the *o*-quinone. Two waves are observed in the cathodic scan. The first wave results from the reduction of the dopamine *o*-quinone, while the second is from the reduction of the aminochrome.

The rate constants for the cyclization reactions were determined by chronoamperometry under conditions of planar diffusion. Potentials steps were made to the diffusion-controlled region of the voltammogram to avoid the complications of the electrode kinetics of the initial two-electron transfer. As shown in Figure 4B, the chronoamperometric current during the oxidation of norepinephrine, converted to an experimental n_{app} by division by the Cottrell equation, approximately doubles at long times ($n_{app} = 1.97 \pm 0.10$, $n = 10$). The value of k for the following chemical reaction was determined with eq 5. Values of k determined at physiological pH are as follows: dopamine, 0.07 ± 0.03 ; norepinephrine, 0.49 ± 0.21 ; epinephrine, $44 \pm 5 \text{ s}^{-1}$ (mean \pm SD, $n = 3$).

(24) Evans, J. F.; Blount, H. N. *J. Am. Chem. Soc.* **1978**, *100*, 4191–4196.

(25) Parker, V. D. *Acc. Chem. Res.* **1984**, *11*, 243–250.

(26) Wipf, D. O.; Wightman, R. M. *J. Phys. Chem.* **1989**, *93*, 4286–4291.

Since for catecholamines the rate-determining step of the DISP1 reaction is the nucleophilic attack of the unprotonated amine on the quinoid ring, the overall rate is pH dependent. Thus, k is given by where k_1 and k_{-1} are the association and

$$k = \frac{k_1 k_2}{k_{-1} [\text{H}^+] + k_2} \quad (6)$$

dissociation rate constants for protonation of the amine and are related by the pK_a , k_2 is the rate constant for the nucleophilic attack, and $[\text{H}^+]$ is the proton concentration. The rate constant for the DISP1 of epinephrine was also determined at pH 6.5 and 8.0. The values of k were 7 and 72 s^{-1} , in accord with the predicted dependence on pH.

Effect of DISP1 on Amperometric Current Spikes Observed at Single Biological Cells. Amperometric detection of catecholamine release from individual adrenal medullary cells appears as a series of successive current spikes. Each spike is due to release from a single vesicle, and its area corresponds to the amount of material that reaches the electrode. The average spike has a width at half-maximum amplitude of 15 ms with the electrode placed $1 \mu\text{m}$ from the cell surface.¹⁵ At least two parameters of interest could contribute to the spike width: the kinetics of secretion from the cell surface and mass transport from the cell surface to the carbon-fiber electrode. In addition, there is time for the DISP1 reaction to occur during each event, which could also affect the temporal width of the spike as well as increase its area.

To evaluate the effect of diffusion on the width of amperometric spikes measured at single cells, we previously developed a finite difference algorithm to describe diffusion of an instantaneous concentration source that originates on a hemispherical surface to an adjacent disk-shaped electrode operated in an amperometric mode.¹⁴ For an instantaneous concentration source that originates in a plane $5 \mu\text{m}$ from the electrode, the spikes are predicted to have a width at half-height of 12 ms, and the width is expected to be 1 ms when the electrode is $1 \mu\text{m}$ from the source. Experimental measurements of spike width agree with these predictions when the electrode is positioned at the more remote distance,¹⁴ but the spikes are not as narrow as predicted with the electrode $1 \mu\text{m}$ from the cell surface.¹⁵

To evaluate the effect of the DISP1 reaction scheme on spike width, the kinetic scheme was incorporated into the finite difference algorithm. For a microelectrode ($r_d = 6 \mu\text{m}$) located $5 \mu\text{m}$ from a hemispherical cell surface, the simulation predicts that DISP1 reaction will increase the spike area and the width at half-height by 24 and 32%, respectively when the rate constant for epinephrine at physiological pH is employed (Figure 5). Increasing the rate constant to the value found for epinephrine at pH 8.2 further increases these two parameters by 6%. In contrast, similar calculations with this electrode positioned $1 \mu\text{m}$ from the cell surface do not show a contribution from the cyclization reaction. Diffusional exit from the gap between the cell and the electrode is sufficiently rapid that the reaction is not observed.

Disproportionation of Catecholamines at Carbon-Fiber Microelectrodes. To evaluate experimentally the effects of the DISP1 electrode at carbon-fiber electrodes, chronoamper-

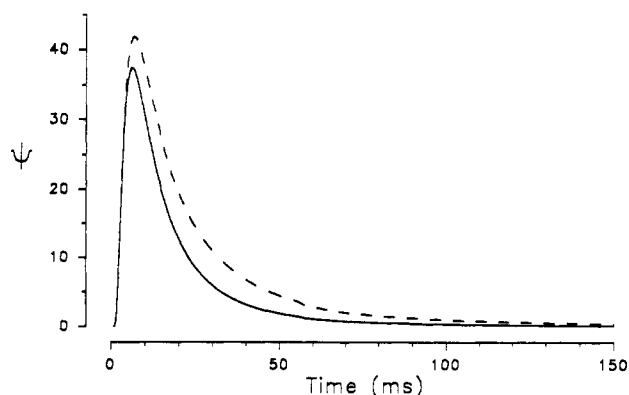


Figure 5. Simulated effect of DISP1 reaction on observed time course of exocytotic release at physiological pH. Adapted from a finite difference algorithm.¹³ Ψ is the dimensionless current. Solid line, simulation in the absence of disproportionation. Parameters, electrode radius, $6 \mu\text{m}$; distance from cell, $5 \mu\text{m}$; diffusion coefficient, $6 \times 10^{-6} \text{ cm}^2/\text{s}$. Dashed line, simulation with DISP1 reaction with k_{obs} , 44 s^{-1} . All other parameters are the same as above.

Table 1. Values of n_{app} Obtained by Chronoamperometry and Cyclic Voltammetry at Carbon-Fiber Microelectrodes of Different Radii^a

method ^b	r_d (μm)	N	n_{app} (mean \pm SD)	simulated n_{app} ^c
CA	2	3	0.95 ± 0.14	1.26
CA	6	13	0.96 ± 0.11	1.52
CA	16.5	6	1.22 ± 0.09	1.75
CV	6	5	1.22 ± 0.07	1.52
CV	16.5	5	1.38 ± 0.08	1.75

^a Solutions contained $40 \mu\text{M}$ epinephrine, pH 7.4. All values were obtained near conditions of steady-state diffusion ($Dt/r_0^2 \approx 100$). ^b CA, chronoamperometry; CV, cyclic voltammetry. ^c Obtained from digital simulation with algorithm for microdisk electrodes with $D = 6 \times 10^{-6} \text{ cm}^2/\text{s}$, $k = 44 \text{ s}^{-1}$.

ometry and cyclic voltammetry of epinephrine were performed under conditions of semiinfinite linear diffusion. The electrodes were disk-shaped carbon-fiber microelectrodes with different radii, and the results are summarized in Table 1. In all cases, the observed value of n_{app} was lower than that predicted by the digital simulation when the rate constant determined from the planar diffusion experiments (44 s^{-1}) was employed. This result is in contrast with that seen with the larger electrode (Figure 4). One possible reason for this discrepancy might be that the simulation is for a disk located on an infinite insulating plane, whereas the actual electrodes employed have insulators of finite thickness. The small dimensions of the insulator could increase the divergence of the diffusion field,²⁷ thereby lowering the observed value of n_{app} . To test for this effect, the insulation thickness of a $6\text{-}\mu\text{m}$ -radius electrode was increased from 1 to $20 \mu\text{m}$. The resulting values of n_{app} (0.99 ± 0.02 , 0.94 ± 0.09 , $n = 5$) were not significantly different.

To determine whether the DISP2 or other second-order mechanisms were operant, the n_{app} values for different epinephrine concentrations were evaluated at a $6\text{-}\mu\text{m}$ -radius carbon electrode. Over the range examined, $0.03\text{--}1 \text{ mM}$, they were invariant.

Another possibility for the low experimental values of n_{app} is that the kinetics of electron transfer are not uniform across the surface of the microelectrode. Prior studies have suggested

(27) Shoup, D.; Szabo, A. *J. Electroanal. Chem.* **1984**, *160*, 27–31.

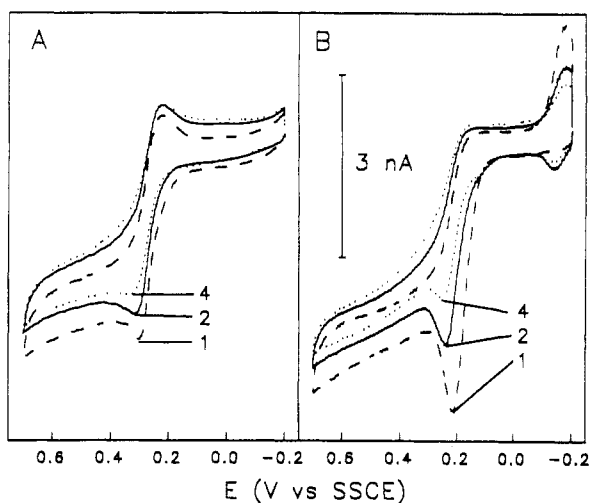


Figure 6. Cyclic voltammograms of catechols obtained at a fractured carbon surface. Scan rate 100 mV/s. The first, second, and fourth scans after fracturing are shown for dihydroxybenzylamine (A) and epinephrine (B). Catechol concentration was 100 μ M in pH 7.4 phosphate buffer.

that the carbon-fiber surface consists of regions of facile electron transfer that are interspersed within regions where electron transfer is sluggish.²⁸ To illustrate the variant nature of the electrode surface, electrodes with radii of 16.5 μ m were prepared and coated with an insulating polymer. The electrodes were placed in solution and the tips were fractured to expose a fresh surface, after which a series of voltammograms were then obtained. Examples are shown for dihydroxybenzylamine, a catecholamine that cannot cyclize when oxidized, and epinephrine in Figure 6. For both compounds, successive scans exhibit lower amplitudes and appear more distorted, indicative of the lower rates of heterogeneous electron-transfer reaction. Note also, in the epinephrine voltammograms, the presence of the leucoaminochrome oxidation wave at the initiation of the second and fourth scans. Since this species is not present in solution, it must have adsorbed to the electrode surface during the prior scans, consistent with the previously reported adsorptive nature of such surfaces.²⁹ The surface of the carbon-fiber, then, is clearly not well-defined, making quantitative treatment of the processes that occur near its surface more complex than with the platinum microelectrodes.

The lack of effect of DISP1 reactions at carbon-fiber electrodes may thus be due to the presence of inactive regions on the carbon surface.²⁹ These will make the apparent rate of reaction appear considerably less than the true rate. This has been illustrated for heterogeneous rate constants at blocked electrodes.³⁰ Then, divergent diffusion can predominate, and the DISP1 process becomes less apparent.

While we have not devised an experimental system to mimic the finite difference simulations, the data suggest that chemical followup reactions do not affect the signals measured at single cells. The experimental results under conditions of semiinfinite diffusion show that the effects of cyclization are less apparent

at carbon-fiber microelectrodes than predicted by the theoretical calculations. These results show that the DISP1 reaction affects the spike width in a negligible way and that instead the width is determined by the kinetics of secretion from the cells. Future investigations will be directed at understanding these biochemical kinetic processes.

ACKNOWLEDGMENT

This research was supported by the grants from the Office of Naval Research and NSF to R.M.W., CNRS-Ultamitech to C.A., and NSF to D.H.E.

Scientific Parentage of the Authors. E. L. Ciolkowski, Ph.D., under R. M. Wightman, Ph.D., under R. W. Murray, Ph.D., under R. C. Bowers, Ph.D., under I. M. Kolthoff.

APPENDIX

The analytical solution for the current during chronoamperometry for an ECE reaction at a spherical electrode,³¹ assuming equal diffusion coefficients for all species and equal numbers of electrons transferred in reactions 1 and 3, is

$$\frac{i}{2nFAD^{1/2}C^*} = \frac{1}{(\pi t)^{1/2}} + \frac{D^{1/2}}{r_0} - \frac{\exp(-kt)}{(\pi t)^{1/2}} + \rho \frac{D^{1/2}}{r_0} \beta$$

where

$$\beta = \left(1 - \frac{D}{r_0^2 \phi^2}\right) \exp(-\phi^2 t) \operatorname{erfc}\left(\frac{Dt}{r_0^2}\right)^{1/2} + \frac{D}{r_0^2 \phi^2} - \frac{(Dk)^{1/2}}{r_0 \phi^2} \operatorname{erf}(kt)^{1/2} - 2 \exp\left(\frac{-kt}{2}\right) I_0\left(\frac{kt}{2}\right) + \frac{4D^{1/2} \exp(-\phi^2 t)}{r_0 (\pm \phi^2 \pi)^{1/2}} \int_0^{\pm \phi^2 t} \exp(\pm \lambda^2) d\lambda - \frac{2D \exp(-\phi^2 t)}{r_0^2} \int_0^t \exp\left(\frac{\tau}{2} \left(k - \frac{2D}{r_0^2}\right)\right) I_0\left(\frac{k\tau}{2}\right) d\tau \quad (7)$$

r_0 is the electrode radius, I_0 is the modified Bessel function, $\rho = n_2/(n_1 + n_2)$, and $\phi^2 = k - D/r_0^2$ (the upper sign applies if $\phi^2 > 0$ and the lower sign applies if $\phi^2 < 0$).

In the limit of $(Dt)^{1/2}/r_0 \ll 1$, this expression reduces to the form found for planar diffusion which, when expressed as the ratio of the chronoamperometric current when kinetics are present to that in the absence of kinetics, n_{app} , is

$$n_{\text{app}} = 2 - \exp(-kt) \quad (8)$$

When $(Dt)^{1/2}/r_0 \gg 1$, eq 7 reduces³²⁻³⁴ to the steady-state solution:

(28) McCreery, R. L. In *Electroanalytical Chemistry*; Bard, A. J., Ed.; Marcel Dekker, Inc.: New York, 1991; Vol. 17, pp 221-374.
 (29) Allred, C. D.; McCreery, R. L. *Anal. Chem.* **1992**, *64*, 444-448.
 (30) Amatore, C.; Saveant, J. M.; Tessier, D. *J. Electroanal. Chem.* **1983**, *147*, 39-51.

(31) Alberts, G. S.; Shain, I. *Anal. Chem.* **1963**, *35*, 1859-1866.
 (32) Fleischmann, M.; Lasserre, F.; Robinson, J. J. *Electroanal. Chem.* **1984**, *177*, 115-127.
 (33) Qiankun, Z.; Hongyuan, C. *J. Electroanal. Chem.* **1993**, *346*, 29-51.
 (34) Oldham, K. B. *J. Electroanal. Chem.* **1991**, *313*, 3356. Oldham, K. B. *J. Electroanal. Chem.* **1981**, *122*, 1-17.
 (35) Oldham, K. B.; Zoski, C. G. *J. Electroanal. Chem.* **1988**, *258*, 11-19.
 (36) Rudolph, M.; Reddy, R. P.; Feldberg, S. W. *Anal. Chem.* **1994**, *66*, 589A-600A.

$$n_{\text{app}} = \frac{r_0(k/D)^{1/2}}{1 + r_0(k/D)^{1/2}} + 1 \quad (9)$$

Between the two extremes expressed by eqs 8 and 9, eq 7 was evaluated with respect to the dimensionless parameters kt and Dt/r_0^2 by use of a commercial software package (MathCAD). Values for n_{app} were obtained by normalization of the calculated current with respect to the spherical form of the Cottrell equation. It was found that the analytical solution could not be evaluated when $\phi^2 = 0$ ($kr_0^2/D = 1$) because four of the terms in the solution go to infinity. Additionally, it could not be evaluated for $kr_0^2/D < 0.02$, i.e., conditions where the following chemical kinetics exert only a small effect on the current.

To extend this result to conditions that are found with microelectrodes, a digital simulation was written to obtain values of n_{app} (with $n_1 = n_2$) for the ECE mechanism at a hemispherical electrode for smaller values of kr_0^2/D . The results were found to be in excellent agreement with the analytical solution (<0.2% error) in the range where the analytical solution could be evaluated and gave the limiting values predicted by eq 9 (Figure 7).

The family of working curves for the ECE mechanism at a spherical electrode (Figure 7) defines a surface that a single chronoamperometric record of n_{app} will traverse. The curves show that at large values of $\log(kt)$ and small values of $(Dt)^{1/2}/r_0$, n_{app} approaches a limiting value of 2 (as in eq 8). The curve for the lowest value of $(Dt)^{1/2}/r_0$ (0.01) is almost identical to that generated from eq 8 while that for $(Dt)^{1/2}/r_0 = 50$ is well represented by the steady-state expression, eq 9. The remaining curves in Figure 7 cover the intermediate region where the effects of sphericity increase with increasing $(Dt)^{1/2}/r_0$ and approach the steady-state solution. In a qualitative sense, for any given n_{app} (e.g., $n_{\text{app}} = 1.5$), the shift of $\log(kt)$ toward larger values as $(Dt)^{1/2}/r_0$ increases represents a competition between the kinetic effect of the ECE reaction (which increases the current) and the divergent spherical diffusion field, which allows the intermediates B and C to escape into bulk solution (which decreases the current). Note that the range over which chemical kinetics are not apparent is extended with larger values of Dt/r_0^2 .

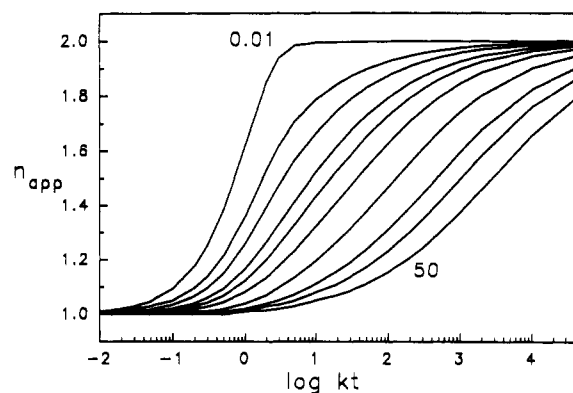


Figure 7. Working curves for the ECE mechanism at a hemispherical electrode. Curves were obtained by digital simulation and are illustrated for $(Dt)^{1/2}/r_0 = 0.01, 0.5, 1, 2, 3, 5, 10, 20, 30,$ and 50 .

For comparison of the ECE and DISP1 mechanisms, k_{obs} is defined as $1/2k$ for the ECE mechanism (eq 8) and as k for the DISP1 mechanism. Under conditions of planar diffusion, the ratio of eqs 8 to 5 shows that the chronoamperometric responses are similar with a maximum difference of 6.5% at $k_{\text{obs}}t = 2.5$. These differences in chronoamperometry remain small when the responses for the DISP1 reaction at a disk (obtained by digital simulation) are compared to the analytical solution for ECE kinetics at a hemispherical electrode (Figure 7). For this comparison, the equivalency of the radii at steady state (disk radius r_d equal to $(\pi/2)r_0^{35,36}$) was employed. Although this equivalency is not appropriate at small values of Dt/r_0^2 , this is not apparent in Figure 2 because the results are expressed as n_{app} . For the experimental conditions considered here ($kr_0^2/D > 0.1$), the error in using the hemispherical ECE model to determine n_{app} for DISP1 kinetics at a microdisk is less than 4%.

Since this work was completed, a commercial simulation package has become available that allows ECE and DISP1 schemes to be compared at spherical electrodes.³⁶

Received for review December 10, 1993. Accepted August 3, 1994.*

* Abstract published in *Advance ACS Abstracts*, September 15, 1994.